A requirement for bone morphogenetic protein-7 during development of the mammalian kidney and eye

Andrew T. Dudley,[1] Karen M. Lyons,[1,2] and Elizabeth J. Robertson[3]

Department of Molecular and Cellular Biology, Harvard University, Cambridge, Massachusetts 02138 USA

BMP-7/OP-1, a member of the transforming growth factor-β (TGF-β) family of secreted growth factors, is expressed during mouse embryogenesis in a pattern suggesting potential roles in a variety of inductive tissue interactions. The present study demonstrates that mice lacking BMP-7 display severe defects confined to the developing kidney and eye. Surprisingly, the early inductive tissue interactions responsible for establishing both organs appear largely unaffected. However, the absence of BMP-7 disrupts the subsequent cellular interactions required for their continued growth and development. Consequently, homozygous mutant animals exhibit renal dysplasia and anophthalmia at birth. Overall, these findings identify BMP-7 as an essential signaling molecule during mammalian kidney and eye development.

The concerted program of cell growth and differentiation during embryogenesis of higher animals is precisely controlled by coordinated cell-cell communication. The formation of many organs and specialized tissues is governed by processes of continuous reciprocal inductive interactions (for review, see Wessells 1977). Although much progress has been made recently in understanding the molecular mechanisms underlying the formation and patterning of discrete embryonic structures such as the vertebrate limb (for review, see Tabin 1995) and Drosophila eye (for review, see Heberlein and Moses 1995), relatively little is known about the components of signaling pathways that guide the growth, morphogenesis, and survival of complex organ systems.

Members of the transforming growth factor β (TGF-β) superfamily of polypeptide growth factors play fundamental roles governing morphogenetic processes throughout embryonic development. For example, in Xenopus activins, Vg-1 and bone morphogenetic protein-4 (BMP-4) are involved in the establishment and subsequent patterning of the mesodermal lineage (for review, see Harland 1994; Kessler and Melton 1994). The Drosophila decapentaplegic (dpp) gene is required for the specification of the embryonic dorsal-ventral axis, midgut morphogenesis, and imaginal disc patterning (for review, see Gelbart 1989; Ferguson and Anderson 1992). Recent

studies have shown that TGF-β family members are essential signaling molecules during early mammalian development. Thus, nodal contributes to the formation and maintenance of the primitive streak in postimplantation mouse embryos (Zhou et al. 1993; Conlon et al. 1994), whereas BMP-4 acts to promote the growth of the embryonic epiblast and mesoderm differentiation (Winnier et al. 1995).

TGF-β superfamily members have been divided into subgroups based on the degree of sequence conservation in their carboxyl-terminal signaling domains. The largest subgroup constitutes the BMPs (for review, see Lyons et al. 1991; Kingsley 1994). The Drosophila dpp and vertebrate BMP-2 and BMP-4 genes are highly conserved and functionally interchangeable (Padgett et al. 1987; Wozney et al. 1988; Padgett et al. 1993; Sampath et al. 1993). The expression patterns described for mammalian BMP-2 and BMP-4 provided early evidence that these molecules promote inductive tissue interactions (Jones et al. 1991; Lyons et al. 1989, 1990). BMP-2 and BMP-4 expressed in the developing vertebrate limb have been shown to function in growth control (Niswander and Martin 1993; Francis et al. 1994) and, during odontogenesis, appear to mediate mesenchymal epithelial interactions (Vainio et al. 1993). A variety of experimental evidence in Xenopus suggests that BMP-4 activity specifies the formation of ventral mesodermal cell types (for review see Harland 1994). The 60A subgroup includes, in addition to the prototypic Drosophila 60A gene, four mammalian genes, BMP-5 to BMP-8, which share 75% homology in their mature carboxy-terminal domains

Dudley et al.

(Özkaynak et al. 1990, 1991; Celeste et al. 1990; Wharton et al. 1991; Rosen and Thies 1992). Loss-of-function alleles of *BMP-5* mapping to the mouse *short ear (se)* locus (Kingsley et al. 1992; King et al. 1994) are associated with defects in specific skeletal elements and soft tissues (Green 1968). However, the developmental roles provided by the closely related *BMP-6* and *BMP-7* family members have yet to be defined.

BMP-7, also referred to as osteogenic protein-1 (OP-1) or DVR-7, was originally identified as a potent osteogenic factor purified from bone (Celeste et al. 1990; Özkaynak et al. 1990). In situ hybridization experiments demonstrate that *BMP-7* mRNA is present at multiple sites during mouse embryogenesis (Lyons et al. 1995). These findings predict several potential roles, including establishment of the notochord at gastrulation and, at later stages, during organogenesis in the formation of the heart, gut, and kidney. To test these possibilities, we have generated a loss-of-function mutation at the *BMP-7* locus. BMP-7-deficient mutants exhibit a number of specific skeletal defects with variable penetrance. Additionally, these animals show striking abnormalities associated with the development of both the renal and ocular systems. Surprisingly, loss of BMP-7 signaling does not disrupt initial reciprocal inductive tissue interactions guiding eye and kidney formation. Rather, the late onset and presentation of renal and ocular defects suggest that BMP-7 may act as a localized growth factor regulating the survival or maintenance of differentiated cell types essential for the maturation of both organs.

Results

Generation of BMP-7 mutant mice

The positive/negative targeting vector used to introduce a null mutation at the BMP-7 locus is shown in Figure 1A. Briefly, an *EagI-HindIII* fragment containing the first coding exon and ~150 bp of upstream sequence was replaced by a PGK–*neo* cassette, in the opposite transcriptional orientation. The *neo* cassette was flanked by ~3.3 and 8.5 kb of 5' and 3' homology, respectively. Linearized vector was electroporated into CCE embryonic stem (ES) cells, and individual colonies selected in G418 and GANC were screened by Southern blot analysis using an external probe. Of 840 drug-resistant clones analyzed, we recovered 107 carrying the mutant allele, and 5 of these were injected into blastocysts. Three independent clones, C2, G6, and F9, gave rise to male chimeras that transmitted the mutation to their offspring. We analyzed *BMP-7* homozygous mutant progeny derived from all three clones to confirm that they all exhibit the identical phenotype. This mutation has been designated $BMP-7^{m1Rob}$.

Southern blot analysis of mid-gestation stage embryos recovered from intercross matings showed that homozygous mutant progeny were recovered at the expected frequency (Fig. 1B). To confirm that the targeted allele encodes a loss-of-function mutation, total RNA from individual embryos was analyzed using an RNase protection assay. As shown in Figure 1C, riboprobes specific for exon 1 sequences and for downstream sequences encod-

Figure 1. Generation of a null allele at the *BMP-7* locus. (*A*) Schematic representation of the wild-type and mutant alleles and the targeting vector. (B) *Bam*HI; (E) *Eag*I; (H) *Hind*III; (R) *Eco*RI restriction sites. (*B*) Southern blot analysis of mid-gestation stage embryos obtained from heterozygous intercrosses. Genomic DNA was digested with *Eco*RI and hybridized with the 5' flanking probe. Positions of the 7.0-kb fragment derived from the wild-type allele and 5.5-kb fragment derived from the mutant allele are indicated. (*C*) RNase protection analysis. A 220-base probe specific for exon 1 and a 202-base probe corresponding to downstream sequences were hybridized with total RNA prepared from mid-gestation embryos. The arrows indicate the positions of the predicted full-length protected fragments detectable in wild-type and heterozygous but not mutant samples. A mouse Sp1 probe was used as a control for mRNA integrity.
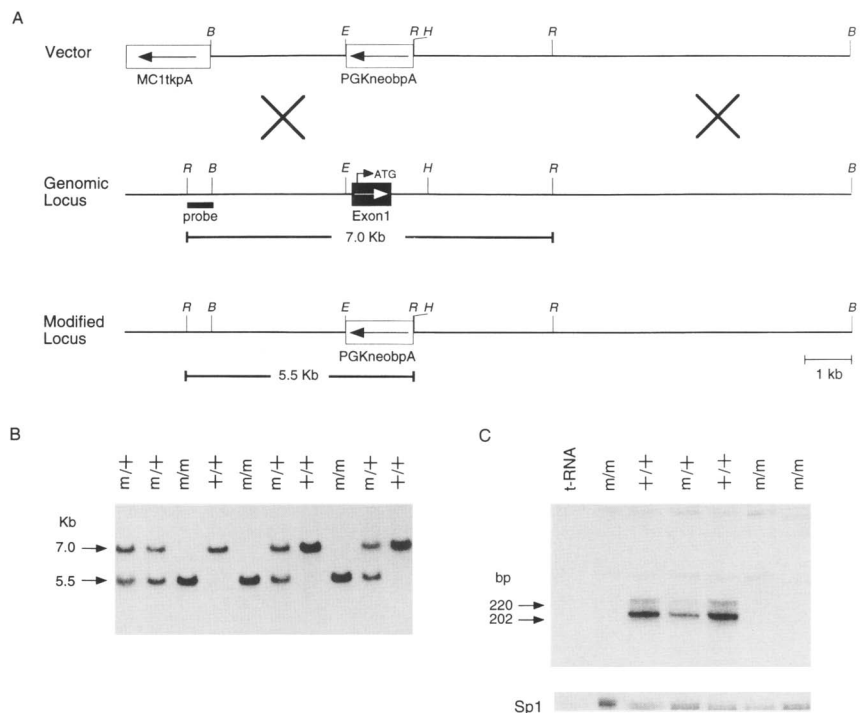
Table 1. *Abnormalities associated with a null mutation at the* BMP-7 *locus*

Sub strain	Litters	Embryos	Mutants (%)	Kidney defects (%)	Eye defects (%)	Hind limb polydactyly (%)
C2	5	39	10 (26)	10 (100)	8 (80)	5 (50)
G6	8	83	18 (20)	18 (100)	18 (100)	2 (11)
F9	5	56	11 (22)	11 (100)	11 (100)	6 (55)
F9 inbred	9	63	14 (22)	14 (100)	14 (100)	1 (7)
Totals	27	241	53 (22)	53 (100)	51 (96)	14 (26)

Embryos recovered between day 16 and 19 of gestation were genotyped as described in Materials and methods. The range in eye defects presented by mutant embryos ranged from bilateral anophthalmia (60%), bilateral microphthalmia (20%), and a combination of unilateral microphthalmia in combination with unilateral anophthalmia (20%).

ing the BMP-7 proregion both gave the appropriate full-length protected fragments upon hybridization with RNA from wild-type or heterozygous animals. In contrast, RNA from several mutant embryos showed no detectable hybridization signal, confirming that these animals lack *BMP-7* transcripts.

Late onset and restricted pattern of abnormalities in BMP-7-deficient embryos

BMP-7 mRNA is expressed at multiple sites in the developing mouse embryo from gastrulation stages onward (Lyons et al. 1995). However, essentially all of the *BMP-7* homozygotes survived to birth, and early postimplantation stage mutant embryos displayed no visible abnormalities. As shown in Figure 2, mid-gestation and later stage *BMP-7* homozygotes were readily identified by their severe eye defects (Fig. 2A,B,E,F). In the majority of cases (60%) this defect presented as bilateral anophthalmia. However, ~20% of mutants, regardless of genetic background, displayed a unilateral microphthalmia in combination with unilateral anophthalmia, whereas the remaining 20% displayed bilateral microphthalmia. Without exception, late gestation and live born mutants also exhibit severe bilateral renal dysplasia (Fig. 2C), often accompanied by massive hydroureter (Fig. 2D). In contrast, the remainder of the urogenital system, gonads, and the adrenals are unaffected (Fig. 2C). The penetrance and expressivity of kidney and eye defects observed in a hybrid (129/Sv × MF1) or an inbred 129/Sv background were not significantly different, suggesting little impact of genetic background on the phenotype. Data obtained analyzing the three independent *BMP-7* mutant strains are summarized in Table 1.

BMP-7 was shown previously to be a potent inducer of bone in ectopic assays (Celeste et al. 1990; Özkaynak et al. 1990) and is widely expressed in developing cartilage and bone (Lyons et al. 1995). In the appendicular skeleton, *BMP-7* mRNA is expressed within the interdigital mesenchyme at mid-gestation stages. Within the axial skeleton, *BMP-7* transcripts are abundant in the developing perichondria. Overall, these findings suggest that *BMP-7* signaling is involved in bone formation and patterning. To examine this possibility further, whole-mount skeleton preparations from 65 animals, including 30 mutants, sacrificed at late gestational or early postnatal stages, were analyzed extensively. Approximately 25% of *BMP-7* mutants displayed unilateral hind-limb polydactyly, seen either as a single additional preaxial digit resembling a mirror image duplication of the second digit or, more rarely, as a bifurcation and duplication of the most distal tarsals of the first digit (Fig.2G,H). Additional minor axial skeletal abnormalities were observed in ~50% of homozygous mutants (16 of 30). The most prevalent defect scored was a failure of one or both of the seventh pair of ribs to fuse to the sternum, often accompanied by the absence of an obvious center of ossification corresponding to the fourth sternebra. Occasionally in the cranial region, the membranous bones were not fully developed, and we recorded two cases of exencephaly.

BMP-7 mRNA is also known to be prominently expressed in other developing organ systems, including the myocardium of the developing heart, the epithelial and mesenchymal layers of the gut, and the epithelial buds of the pancreatic primordium (Lyons et al. 1995; Vukicevic et al. 1994). However by histological criteria, all of these tissues appear to develop normally. The vast majority of *BMP-7* mutants die within the first day of postnatal life, probably because of renal failure. However, a small percentage of mutants (~5%) survive for 2–10 days. Although these animals appeared runted, they developed a normal pelage and displayed normal behavior. On autopsy, they were all found to have severely dysplastic kidneys and accompanying hydroureter.

Defective kidney development caused by loss of BMP-7 function

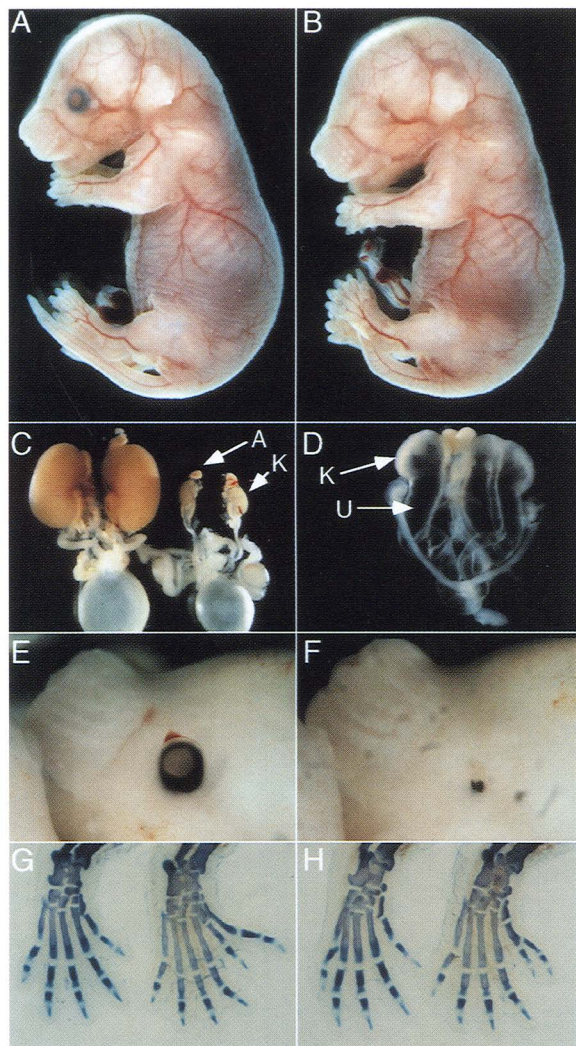Overt development of the metanephric kidney is initi-

Dudley et al.

Figure 2. Gross morphological analysis of *BMP-7* mutant embryos. Adjacent panels photographed at the same magnification showing heterozygous (*A*) and homozygous mutant (*B*) littermates at 17 days p.c. (*C*) At 19 days p.c., kidneys (*k*) from *BMP-7* mutant embryos (*right*) are significantly smaller than those from a heterozygous littermate (*left*). The remainder of the urogenital tract and adrenals (K) are morphologically normal. (K) kidney. (*D*) Acute hydroureter phenotype displayed by the majority of BMP-7 mutants at birth. A small mass of kidney tissue remains (K), while the renal pelvis (R) and ureter (U) are extremely distended (*E,F*) High magnification views of eyes at 13.5 days p.c. The wild-type embryo (*E*) shows a well-developed pigmented retinal epithelium, whereas the *BMP-7* mutant embryo (*F*) has only a residual mass of pigmented retinal epithelial cells. (*G,H*) Preaxial polydactyly of the hind limbs. Whole-mount preparations comparing the cartilaginous structures present in wild-type (*left*) and BMP-7 mutant (*right*) limbs are shown.

ated, beginning at ~11 days of development, by growth of the Wolffian duct-derived ureteric bud into the presumptive metanephric mesenchyme. Subsequent reciprocal interactions result in branching morphogenesis of the ureteric bud and conversion of the induced mesen-

chyme into epithelial structures. These primitive structures subsequently differentiate into epithelial components of the mature nephron, whereas derivatives of the ureter form the collecting duct system (for review, see Saxen 1987). *BMP-7* transcripts are initially detected in the mesonephric duct and tubules at 9.5 days of development (Lyons et al. 1995). Following formation of the metanephric kidney, *BMP-7* transcripts are prominently expressed in the mesenchyme of the nephrogenic zone, the condensing aggregates, and the epithelia of the comma and S-shaped pretubular structures, with weaker expression seen in the ureteric ducts (Fig. 3A). Moreover, *BMP-7* mRNA expression persists in the nephrogenic zone throughout development, and *BMP-7* transcripts are readily detectable in adult kidneys (Özkaynak et al. 1991).

To determine the onset of abnormalities during kidney development, the structures of mutant and wild-type kidneys were carefully compared over time. There were few distinctive morphological differences observed prior to day 14.5. A detailed histological analysis of day 14 mutant kidneys showed a relatively normal architecture, with prominent branching of the ureteric buds (Fig. 3D). Moreover, comma and S-shaped bodies are present, strongly suggesting that the reciprocal inductive interactions necessary to initiate and promote growth and differentiation of the developing nephrons have occurred in the absence of *BMP-7* signaling (Fig. 3C). However, organ size and the overall extent of nephrogenesis is reduced markedly in BMP-7 mutants, resulting in the accumulation of a disproportionately higher amount of loose interstitial mesenchyme (Fig. 3D). Over the next 2 days, BMP-7-deficient kidneys acquire a highly aberrant, disorganized architecture (Fig. 3F). Moreover, there is little morphological evidence for active formation of mesenchymal aggregates. The peripheral layer is largely devoid of densely packed mesenchymal stem cells, and medullary regions are typically filled with large numbers of collecting ducts interspersed by loose stromal cells.

Next we assessed kidney development using a panel of specific molecular markers. To determine the extent of ureteric bud branching, we analyzed the expression of the c-ret receptor tyrosine kinase. c-ret mRNA is specifically expressed within the tips of the newly formed branches of the ureteric buds at the periphery of the kidney (Pachnis et al. 1993). To evaluate the state of induction and differentiation of the metanephric mesenchyme, we examined *Pax-2*, *Pax-8*, and *Wnt-4* expression. *Pax-2* and *Pax-8* are members of the paired domain class of transcription factors (Walther et al. 1991). *Pax-2* mRNA is initially found in the mesonephric duct, and then in the branching ureter, induced mesenchymal condensates, and S-shaped bodies (Dressler et al. 1990), whereas, *Pax-8* expression is restricted to the induced mesenchyme and S-shaped bodies (Plachov et al. 1990). *Wnt-4* expression is required for epithelialization of the induced mesenchyme (Stark et al. 1994) and thus serves as a marker for formation of pretubular aggregates and comma-shaped bodies. As shown in Figure 4, at day 14.5, BMP-7-deficient kidneys express all of these markers in
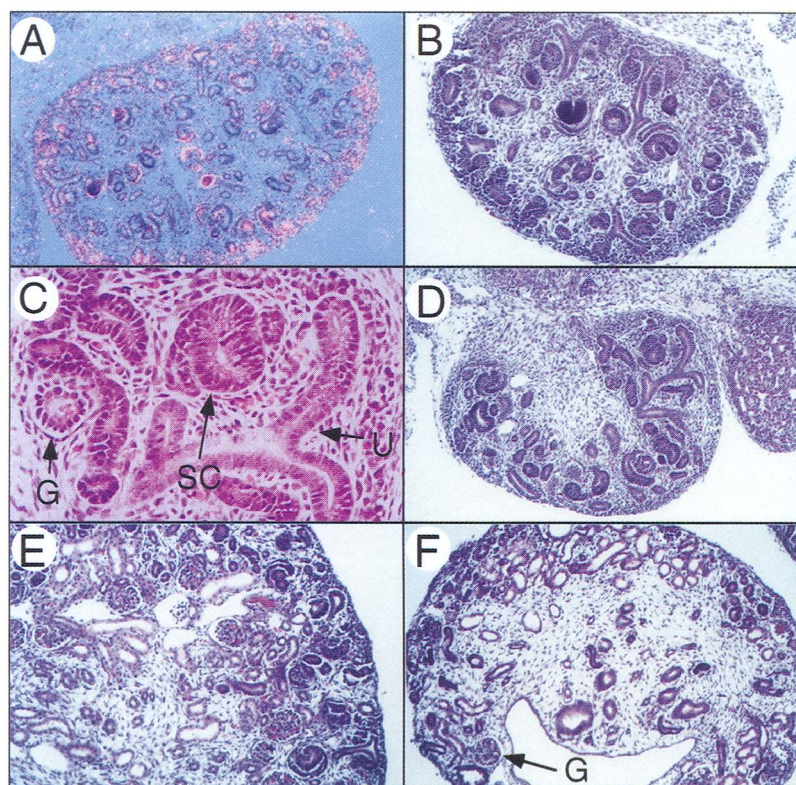
Figure 3. Kidney abnormalities associated with the absence of *BMP-7* expression at later stages of development. (*A*) Abundant levels of *BMP-7* transcripts are detected in the mesenchymal stem cells, condensing aggregates, and Bowman's capsule of wild-type kidneys at 14.5 days of development. Sections through wild-type (*B*) and mutant (*D*) kidneys at 14.5 days p.c. were photographed at the same magnification (200×). (*C*) High magnification (600×) view of the upper right quadrant of *D*. Views of wild-type (*E*) or mutant (*F*) kidneys at 16 days p.c. photographed at 200× magnification. (G) Glomerulus; (SC) S- or comma-shaped body; (U) ureter.

an appropriate cell type-specific pattern. These findings suggest that the absence of BMP-7 signaling has little impact on the inductive interactions between the epithelial and mesenchymal tissues during early kidney formation. However, this expression study illustrates a dramatic reduction in the extent of branching morphogenesis, mesenchymal condensation, and epithelialization in the absence of BMP-7 signaling.

As expected, at 16.5 days post coitum (p.c.), expression of *c-ret*, *Pax-2*, *Pax-8*, and *Wnt-4* persists in the cortex of wild-type kidneys, indicating ongoing nephrogenesis. In contrast, mutant kidneys are largely devoid of these cell populations (Fig. 5). As predicted by the drastically reduced branching of the ureter, we observed occasional patches of *c-ret*- positive cells. Similarly, small clusters of *Pax-2*-, *Pax-8*- and *Wnt-4*-expressing cells were found associated with small poorly formed mesenchymal aggregates. In contrast, in the medullary regions of mutant kidneys, epithelial cells of the collecting ducts derived from the ureter appear to develop normally. High levels of both *Pax-2* and *Wnt-4* transcripts were present in these cell populations.

At later stages of development mutant kidneys are greatly reduced in size in comparison to wild type, severely dysgenic, and contain few recognizable glomeruli and nephrons. Despite this highly aberrant organ structure, the few nephrons that form seem to be functional, as the bladders of live born mutant animals contain filtrate. Postnatal survival of exceptional mutant animals also strongly argues that limited renal function is re-

tained. The homozygous mutants also display severe hydroureter, encompassing massive distension of the collecting ducts, renal pelvis, and ureter (Fig. 2D). The rest of the urinary tract appears to be unaffected. However, we cannot exclude the possibility that minor structural defects attributable to the loss of *BMP-7* function may contribute to the acute hydroureter.

An essential role for BMP-7 in eye development

During the development of the vertebrate eye, the optic vesicle, an outpocketing of the ventral diencephalon, contacts the adjacent surface ectoderm to induce the formation of the lens placode. Coincident with invagination of the lens vesicle, the epithelium of the optic vesicle forms a bilayered optic cup around the newly induced lens vesicle. As a result of secondary inductive interactions, these tissues then act in concert to form the outer and inner cell layers corresponding to the pigmented retinal epithelium and neural retina, respectively (for review, see Grainger 1992). *BMP-7* transcripts are expressed in both the neuroepithelium of the optic vesicle and the overlying surface ectoderm at early stages of eye development (Fig. 6A; Lyons et al. 1995). Following lens induction and formation of the bilayered retina, *BMP-7* mRNA is abundantly expressed at the junction between the neuroepithelium and pigmented retinal epithelium, throughout the outer pigmented retinal layer, in the mesenchymal cells adjacent to the optic cup and
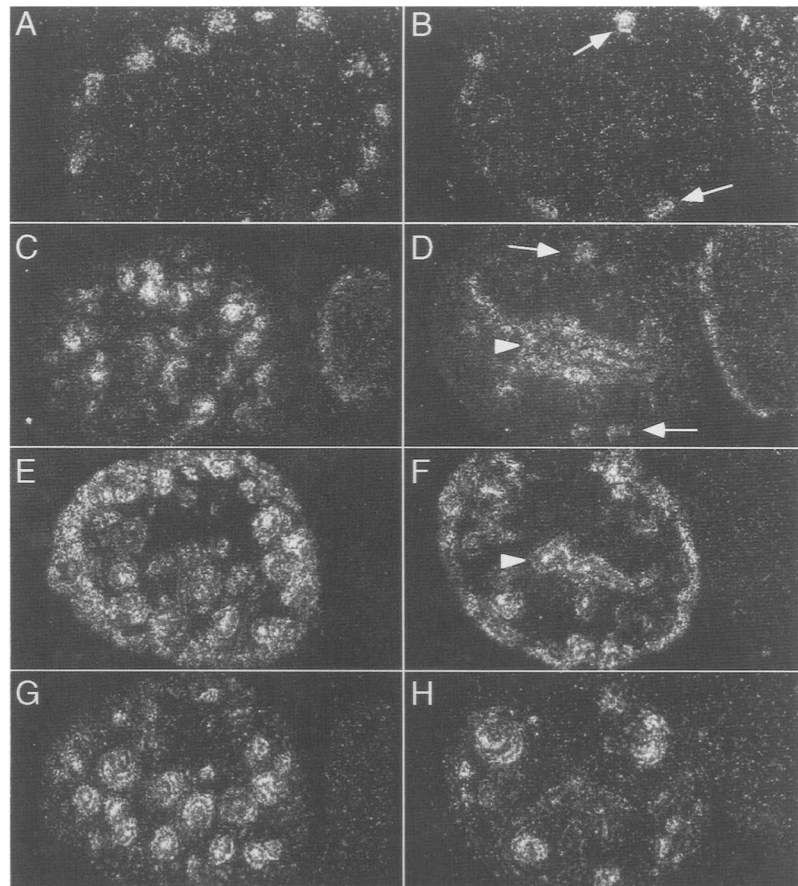
Figure 4. Ureteric bud and mesenchymal cell populations develop normally in BMP-7-deficient kidneys. Dark-field photomicrographs showing expression of *c-ret* (*A,B*), *Wnt-4* (*C,D*), *Pax-2* (*E,F*), and *Pax-8* (*G,H*) transcripts at 14.5 days p.c. in kidneys from wild-type (*A,C,E,G*) and mutant (*B,D,F,H*) embryos. Arrows indicate expression of *c-ret* in the tips of the ureteric buds (*B*) and *Wnt-4* transcripts present in the condensing mesenchyme (*D*) of mutant embryos. Strong expression of *Wnt-4* (*D*) and *Pax-2* (*F*) in or near the collecting ducts is shown by the arrowhead. The mutant and wild-type kidney tissues were embedded and processed in the same specimen block and photographed at the same magnification.

lens (see Fig. 6B), and sheath cells surrounding the optic nerve (data not shown).

We carried out a detailed histological analysis to assess the extent of eye development in *BMP-7* mutant embryos. Considering that lens induction is the primary event responsible for subsequent growth and development of non-neural eye structures, the simplest possibility was that defects in this early phase of eye development might underlie the anophthalmia in *BMP-7* mutants. Tissue sections from three litters of 9.5 day embryos (n = 25) were scored for eye induction and retrospectively genotyped. As shown in Figure 7, induction of the lens placode and invagination of the lens vesicle occurs in BMP-7 mutants (n = 6). Moreover, wild-type and mutant optic stalks appear indistinguishable through day 11 of development. Thus, the competence of the surface ectoderm to respond to signals from the optic vesicle and early patterning of these tissues appears unaffected in the absence of BMP-7 signaling.

By 14.5 days, the majority (60%) of BMP-7 deficient embryos exhibit a profound bilateral deterioration of the developing eye structures. As shown in Figure 8, at this stage the only recognizable eye tissue is a small mass of disorganized pigmented retinal epithelium associated with the remnant of the optic nerve. Interestingly, the remaining 40% of mutants display either unilateral or bilateral microphthalmia. These eyes appear grossly morphologically normal but are approximately half the normal size (Fig. 9). In both anophthalmic and microphthalmic mutants, the tissues of the eyelids develop normally and have fused at birth. Previously described mutations affecting eye development are commonly accompanied by additional craniofacial abnormalities. For example, *Pax-6* mutations mapping to the mouse *small eye* (*Sey*) locus (Hill et al. 1991) disturb development of both the optic and nasal structures (Hogan et al. 1988; for review, see Glaser et al. 1995). In contrast, here the eye was the only grossly affected head structure (Fig. 8).

To describe specific cell types present in these highly degenerate eye rudiments and microphthalmic eyes, next we assessed expression of a panel of molecular markers. The homeo box-containing gene *msx-1* is expressed after formation of the optic cup in cells of the ciliary body, progenitors of the definitive iris located at the extreme tips of the neural retina (Monaghan et al. 1991). In microphthalmic eyes *msx-1* expression was restricted to the ciliary body, consistent with normal organization of this structure (Fig. 9H), whereas *msx-1*-expressing cells were undetectable in degenerate eyes. As mentioned above, Pax-6 expression is essential for lens placode formation (Hogan et al. 1988). *Pax-6* transcripts are initially expressed in both the optic vesicle and the overlying surface ectoderm (Walther and Gruss 1991; Grindlet et al. 1995), whereas at later stages, *Pax-6*
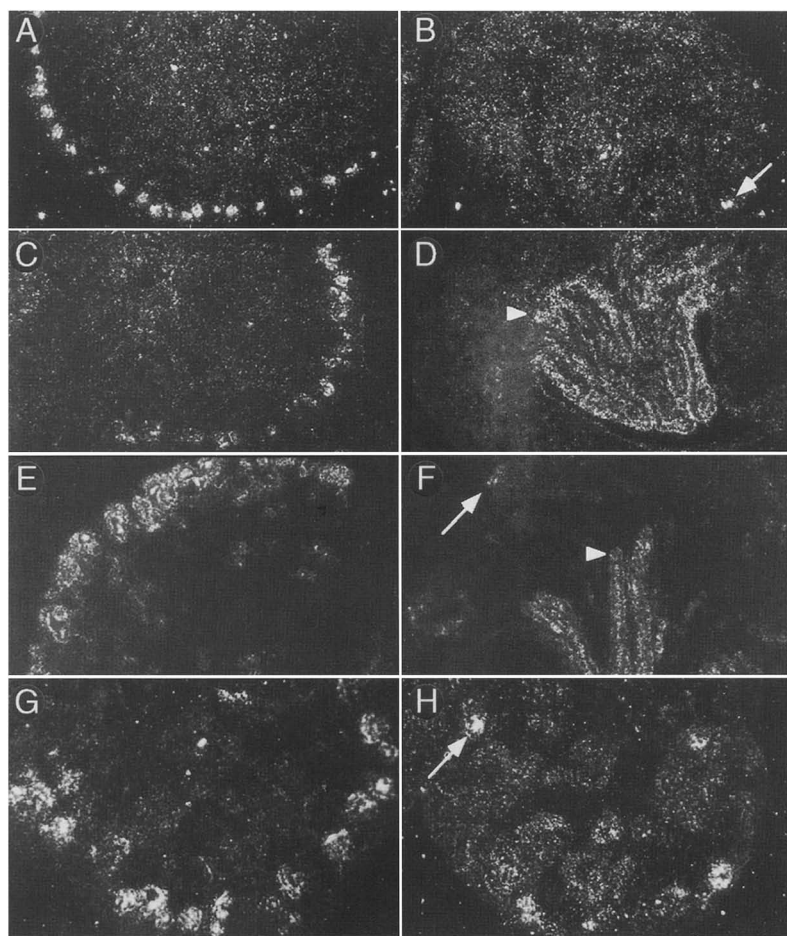
Figure 5. Expression of cell type-specific markers in *BMP-7* mutant kidneys at 16.5 days p.c. Probes specific for *c-ret* (*A,B*), *Wnt-4* (*C,D*), *Pax-2* (*E,F*), and *Pax-8* (*G,H*) were hybridized to wild-type (*A,C,E,G*) and mutant (*B,D,F,H*) tissue sections. Arrows indicate regions expressing *c-ret* (*B*), *Pax-2* (*F*), and *Pax-8* (*H*) transcripts. Note the relatively high levels of *Wnt-4* (*D*) and *Pax-2* (*F*) expression in the collecting ducts of mutant kidneys (arrowheads). The mutant and wild-type kidney tissues were embedded and processed in the same specimen block and photographed at the same magnification.

mRNA is expressed in the developing lens, throughout the neuroepithelium of the developing retinal layers, and in prospective corneal cells derived from the surface ectoderm. An appropriate pattern of *Pax-6* mRNA expression was observed in microphthalmic eyes (Fig. 9E). Previous findings suggest that the maintenance of *Pax-6* expression in the corneal layer is dependent on lens induction, as this expression domain is absent in *Sey* homozygotes lacking a lens placode (Grindley et al. 1995). We found a superficial layer of *Pax-6*-expressing cells present in degenerate eyes, strengthening the notion that lens vesicle formation occurs in the absence of BMP-7 signaling (Fig. 9F). Finally, the finding of residual disorganized pigmented epithelial cells normally formed at day 11 of development provides further evidence that the initial inductive tissue interactions are unaffected. However, as in the developing kidney, BMP-7 activity seems to be essential to promote later stages of organogenesis. Thus, subsequent outgrowth and survival of eye structures are severely impaired and the optic cup and associated optic nerve are not maintained.

Discussion

BMP-7/OP-1, is expressed at early stages of postimplantation mouse development, and moreover is localized to tissues such as the notochord and surface ectoderm, known to participate in inductive tissue interactions. It therefore seemed likely that *BMP-7* mutants might display abnormalities affecting axial patterning as has proven to be the case for other TGF-β family members expressed during gastrulation such as *nodal* and *BMP-4* (Zhou et al. 1993; Conlon et al. 1994; Winnier et al. 1995). Surprisingly, axis formation, neural patterning, and gut development all appear to occur normally in embryos lacking BMP-7. Rather *BMP-7* mutants predominantly display abnormalities confined to the developing kidney and eye. The absence of BMP-7 signaling fails to disrupt early inductive tissue interactions responsible for establishing these organs. However, the absence of BMP-7 signaling causes the loss of their continued growth and differentiation. The late onset and restricted pattern of tissue abnormalities in mutant animals seem especially curious in light of the early pattern of *BMP-7* expression in developing mouse embryos. It is possible that maternal sources of BMP-7 promote early development of early postimplantation-stage embryos. Alternatively, overlapping expression of closely related TGF-β family members may rescue gastrulating embryos.

As predicted by *BMP-7* expression restricted to perichondrial regions in these structures, minor defects af-
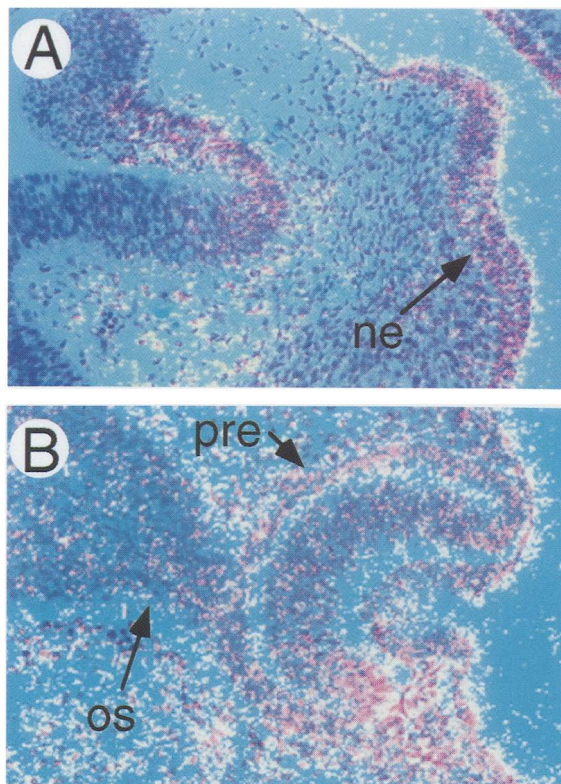
Dudley et al.

Figure 6. Expression of *BMP-7* mRNA in the developing eye. Tissue sections at 9.5 (*A*) and 10.5 (*B*) days of development were hybridized with a BMP-7 specific probe. At 9.5 days p.c. *BMP-7* mRNA expression is localized to the cells of the surface ectoderm and the neuroepithelium of the optic vesicle. Following development of the optic cup, high levels of *BMP-7* transcripts are present in the pigmented retinal epithelium, presumptive ciliary body of the bilayered retina, and in the cells surrounding the optic stalk. (ne) Neural ectoderm; (pre) pigmented retinal epithelium; (os) optic stalk.

fecting the development of the ribs were detected in *BMP-7* mutant embryos (Lyons et al. 1995). The relatively mild nature of the axial skeletal defects may reflect overlapping expression of other TGF-β family members (Lyons et al. 1995; data not shown). During limb development, *BMP-7* transcripts are expressed at high levels in the interdigital mesenchyme, which normally undergoes programmed cell death. The appearance of extra digits in *BMP-7* mutants could in principle reflect a role for BMP-7 in mediating apoptosis during limb development, as seems to be the case for BMP-4 signaling in the chick hind brain (Graham et al. 1994). Alternatively, if BMP-7 normally acts to inhibit cell growth, its absence may lead to an expansion of the limb field and formation of additional digits.

BMP-7 is expressed in multiple cell types during ontogeny of the metanephric kidney. Thus, *BMP-7* transcripts are present in cells of the ureter and the metanephric mesenchyme. Following condensation of the mesenchyme into pretubular aggregates, *BMP-7* expres-

sion continues in the resulting comma and S-shaped bodies. A continuous program of reciprocal inductive epithelial mesenchymal interactions is responsible for the formation of functional nephron units and the overall structure of the mature kidney (for review, see Saxen 1987). Mutations affecting either the ureteric component or the metanephric mesenchyme are sufficient to disrupt the nephrogenic program. For example, the c-ret receptor, expressed in the tips of the ureteric buds, is essential for branching morphogenesis (Schuchardt et al. 1994), and a secondary effect of the mutation is the failure of the uninduced mesenchyme to proliferate. Mutants lacking *c-ret* survive to birth and either lack kidneys or display small dysplastic rudiments. Similarly, loss of the *Wnt-4* signaling molecule specifically blocks the inductive process responsible for conversion of mesenchymal aggregates into tubules (Stark et al. 1994). *Wnt-4* mutants fail to develop recognizable glomeruli, and kidney growth is arrested at day 15 of development. In contrast, here, initial epithelial–mesenchymal inductive interactions appear largely unaffected. Thus, we observed morphologically normal mature nephrons at day 14.5. However, the coordinated program of cell growth and differentiation is not maintained. Starting prior to day 14 we observe greatly reduced branching morphogenesis of the ureter accompanied by a decrease in the formation of associated pretubular aggregates. We therefore conclude that BMP-7, acting either in an autocrine or paracrine fashion, is necessary to promote the continued growth
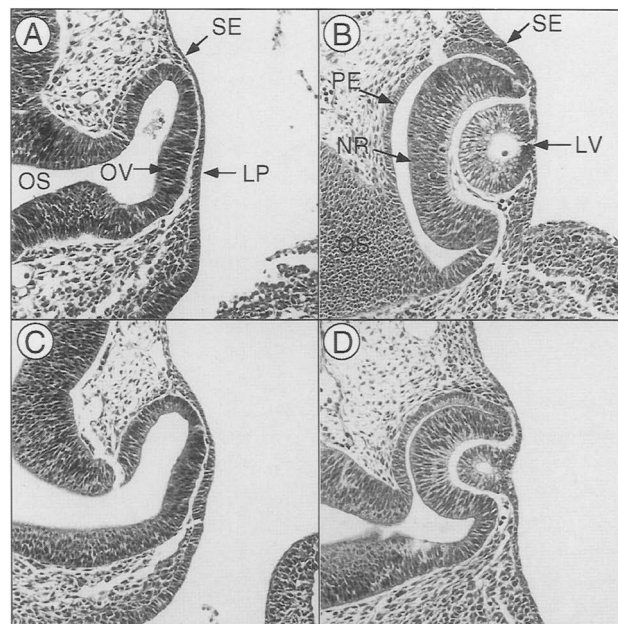

Figure 7. Lens induction in the absence of BMP-7 signaling. Frontal sections through 10 days p.c embryos showing formation of the surface ectoderm-derived lens placode (*A,C*) and lens vesicle (*B,D*) in wild-type (*A*), heterozygous (*B*) and mutant (*C,D*) embryos. (LP) Lens placode; (LV) lens vesicle; (NR) neural retina; (OS) optic stalk; (OV) optic vesicle; (PE) pigmented epithelium; (SE), surface ectoderm.
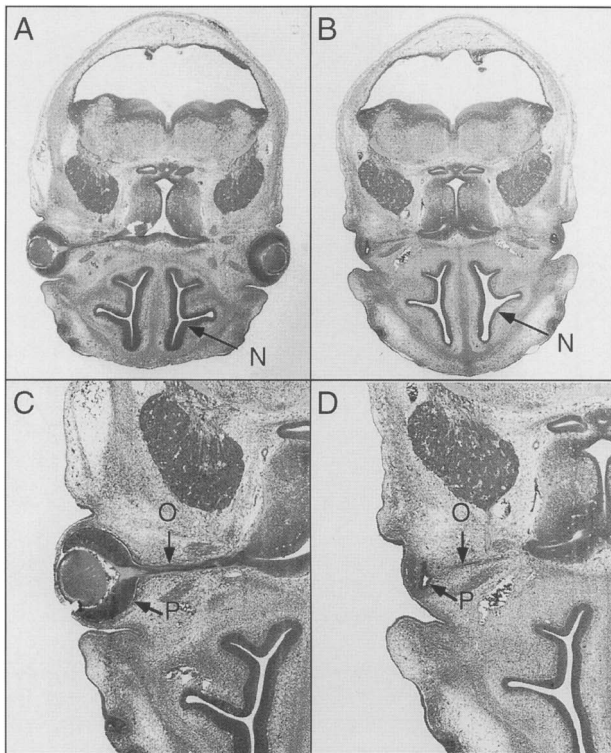
Figure 8. Defective eye development in BMP-7 mutants. Hematoxylin- and eosin-stained sections through the head region of 14.5 days p.c. wild-type (A,C) and BMP-7 mutant (B,D) embryos. Note the presence of a nasal cavity (N) in mutant embryos. Higher magnification views are shown in C and D. Note the remnant of the pigmented epithelium (P) and optic nerve (O) in the mutant. Mutant and wild-type tissues were embedded and processed in the same specimen block and photographed at the same magnification.

and survival of both epithelial and mesenchymal components in the developing metanephric kidney. Perhaps BMP-7 is essential to promote continuous branching morphogenesis of the ureteric bud. Alternatively, BMP-7 may act to maintain the proliferation of mesenchymal stem cell populations occupying the nephrogenic zone or affect the competence of this population to convert to pretubular condensates. Extensive cell death seems to be a feature of normal kidney development (Koseki et al. 1992; Coles et al. 1993) and is apparently blocked by the actions of growth factors such as epidermal growth factor (EGF) (Coles et al. 1993). One possibility is that BMP-7 specifically promotes the survival of these discrete cell types. Interestingly, in contrast, recent data suggest that BMP-4 mediates apoptosis in specific populations of neural crest derivatives in the chick (Graham et al. 1994).

In the developing eye, BMP-7, like Pax-6, is expressed in both the inducing optic vesicle and the responding surface ectoderm. In contrast to the phenotype described for Pax-6 mutants, here the primary induction of the lens placode and vesicle occurs normally. Moreover, the persistence of Pax-6 expression in prospective corneal cells

provides strong evidence for lens induction (Grindley et al. 1995). Similarly, development of the pigmented retinal epithelial layer in mice lacking BMP-7 strongly suggests that optic cup formation proceeds relatively normally. Nonetheless, the majority of mutants show rapid and extensive deterioration of the eye and associated optic nerve. Thus, BMP-7 provides an essential function in maintaining the integrity of optic structures. Similar tissue abnormalities have been described for spontaneous mouse mutations affecting the eye. For example, the semidominant (Sey) mutation affecting Pax-6 expression (Hill et al. 1991), results in a failure to induce the lens placode (Hogan et al. 1988). As a secondary consequence, development of the optic cup is disturbed leading to loss of this structure and the associated optic nerve. Interestingly, Sey heterozygotes develop microphthalmia, possibly because of a temporal delay in the invagination of the lens vesicle (Theiler et al. 1978). Similarly 90% of eyeless homozygous mice are bilaterally anophthalmic whereas the remaining 10% develop microphthalmia (Chase and Chase 1941). The predominant factor determining the severity of the phenotype appears to be the size of the lens vesicle and its positioning relative to the optic cup (Harch et al. 1978). When the lens is centered correctly a small eye develops, whereas in other animals the poorly positioned lens is lost, and the optic cup collapses and degenerates. Thus, BMP-7 signaling may be required to guide growth and appropriate positioning of the lens vesicle and cells of the neuroepithelium. High levels of BMP-7 mRNA expression are detected in the cells of the early optic stalk at day 10.5 of development, with expression persisting in the cells immediately surrounding the forming optic nerve. Thus, eye degeneration in BMP-7 mutants may also arise as a secondary effect attributable to abnormalities in the optic stalk or nerve. In rats experimental lesion of the optic nerve causes apoptotic cell death of retinal cells (Rabacchi et al. 1994). An association between aplasia of the optic nerve and microphthalmia has also been implicated by studies analyzing the ocular retardation (or) mutation in the mouse (Silver and Robb 1979). BMP-7 might therefore act as a localized trophic factor promoting the survival of neural cell populations in either the retina or associated optic nerve.

Finally, hereditary abnormalities affecting both eye and kidney development have been described previously in humans and mice. Pax-2 mutations in the human population have impacts on both kidney and eye development (Sanyanusin et al. 1995). Moreover, the spontaneous mutation eye blebs, causing defects affecting the kidney and eye, is associated with polydactyly (Lyon and Searle 1989). It will be interesting to learn whether any of the defects presented in these mutations may result, in part, from alterations in BMP-7 expression. The present experiments demonstrate an essential role for BMP-7 signaling during eye and kidney development. In both cases, the inductive tissue interactions responsible for early patterning appear relatively intact, but the absence of BMP-7 dramatically affects overall organ size. These findings suggest that coordinated programs of eye
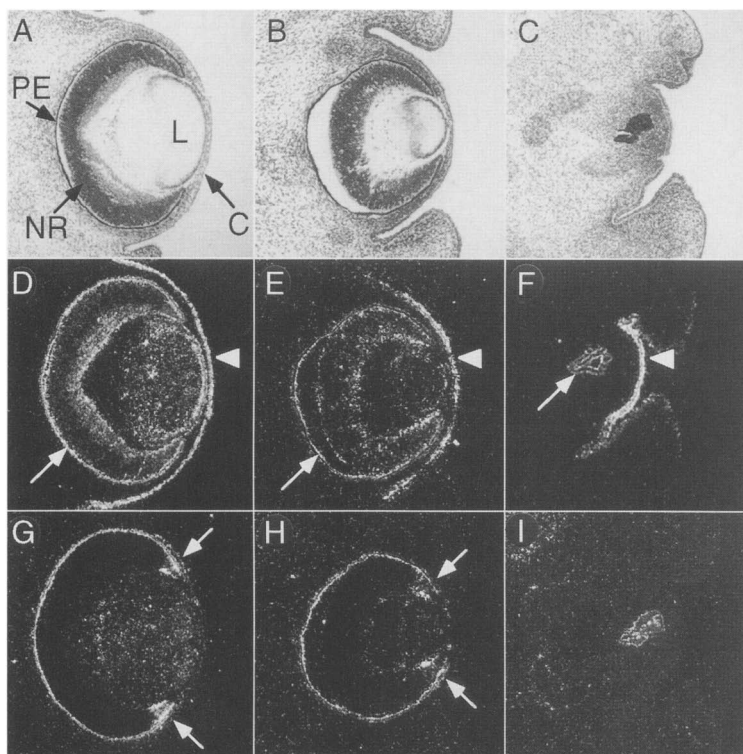
Figure 9. Cell type-specific markers expressed in the developing eyes of BMP-7 mutant embryos. Bright-field (A–C) and dark-field photographs (D–I) of tissue sections through the eyes from wild-type (A,D,G), microphthalmic (B,E,H), and anophthalmic (C,F,I) mutant embryos at 13.5 days p.c. All panels are photographed at the same magnification. Pax-6 (D–F), and Msx-1 (G–I)-specific probes were hybridized to tissue sections. The presence of pigment granules gives an apparent signal seen in the pigmented retinal epithelium, indicated by the arrows in D–F, which serves to delineate the extent of development of this cell layer. Pax-6 expression in D–F (arrowhead) corresponds to cells of the prospective corneal layer. msx-1 mRNA was present in the ciliary body in both wild-type (G) and microphthalmic (H) eyes (arrows). (C) Cornea; (L) lens; (NR) neural retina; (PE) pigmented epithelium.

and kidney development could in principle be dependent on a common signaling pathway activated by BMP-7.

BMPs are phylogenetically conserved and occupy a unique position within the TGF-β superfamily. Members of both subgroups possess the ability to induce formation of ectopic cartilage and bone, suggesting a high degree of functional redundancy. Moreover, recent studies have demonstrated that BMP signaling in mammalian cells involves cooperative interactions between type I and type II receptors as shown for pairs of type I and type II TGF-β receptors (Liu et al. 1995). Interestingly BMPR-II, expressed in mammalian cells, associates with BMP and not TGF-β or activin type I receptors, raising the possibility that BMP ligands can initiate a distinct signaling pathway (Liu et al. 1995). Within the BMP subfamily however, all previous studies analyzing cultured cell lines have failed to discriminate their biochemical and functional activities. Moreover, BMP-2 and BMP-7 have overlapping expression patterns in vivo (Lyons et al. 1995) and BMP-2, BMP-4, and BMP-7 appear to interact with common type II receptors (Liu et al. 1995; Rosenzweig et al. 1995; Yamashita et al. 1995). Nevertheless mutant mice lacking BMP-4 (Winnier et al. 1995) and BMP-7 ligands display remarkably different phenotypes. Further analysis of these animals and compound mutants may provide additional insight into the distinct and overlapping roles of these various BMP family members.

Materials and methods

Derivation of mutant mice

A fragment of the mouse BMP-7 cDNA (Lyons et al. 1995) was used to screen a 129/Sv genomic library. Genomic clones were mapped, and a 1.2-kb EagI–HindIII fragment was identified as containing the first 525-bp coding exon. To construct a positive/negative targeting vector, a 3.3-kb BamHI–EagI fragment located 5′ to exon I was subcloned into the NotI site of pPGK–neo-tk (gift from Brian Parr, Harvard University, Cambridge, MA), 3′ to the neo cassette. An 8.5-kb HindIII–BamHI genomic fragment was subcloned into the vector 5′ to the neo cassette. In the final vector configuration of the PGK–neo cassette replaced exon 1 sequences, and the tk counterselection cassette was positioned 5′ to the 3.3-kb genomic fragment.

CCE ES cells (2×10^7) (Robertson et al. 1986), maintained on STO–neo feeder cells, were electroporated with 15 µg of SalI-linearized plasmid, plated, and selected in G418 (200 µg/ml) and Gancyclovir (2 µM) as described previously (Poirier and Robertson 1993). Drug-resistant colonies were picked into 96-well plates and screened by Southern blot analysis using the procedure described by Ramirez-Solis and colleagues (1993). DNA samples were digested with EcoRI, resolved on 0.7% agarose gels, blotted onto Hybond N membranes (Amersham), and probed using a 0.7-kb EcoRI–HindIII genomic fragment derived from sequences located 5′ to the targeting vector. Correctly targeted ES cell clones were injected into C57BL/6J host blastocysts to generate chimeric animals as described (Bradley 1987). Male chimeras were bred with C57BL/6J or MF1 females to ascertain germ-line transmission. Germ-line chimeras from the F9 ES clone were also mated to 129/Sv//Ev females to generate mutants on an inbred background.

Genotyping procedures

F_1 progeny heterozygous for the mutation were identified by Southern blotting of 10 µg of genomic DNA samples using the procedure described above. Subsequent progeny and embryos were genotyped either by Southern blot analysis or by PCR. The PCR primers were designed to use a common 5′ primer, specific

for sequences located 5' of exon 1 (5'-GCCCGGGCCAGAAC-TGAGTAAA-3'), in conjunction with a primer specific for the *neo* gene (5'-GGTGCCCACTCCCACTGTCCT-3') or for *BMP-7* exon 1 sequences (5'-CGTCCACGACCCGAGGT-CACTT-3') to generate 130-bp and 120-bp products specific for the mutant and wild-type alleles, respectively. The PCR conditions were 50 mM KCl, 10 mM Tris-HCl at pH 7.5, 10% glycerol, 0.25 μM each primer, 1 μg of genomic DNA, and 1 unit of Amplitaq (Perkin-Elmer), in a 25-μl total reaction volume. Following an initial denaturation step (94°C for 1 min), samples were subjected to 30 amplification cycles (94°C for 30 sec, 62°C for 30 sec, 72°C for 30 sec). The amplification products were separated on a 1.5% agarose gel and visualized following ethidium bromide staining.

RNase protection analysis

Total RNA was isolated from 14.5 day p.c. embryos using the guanidinium thiocyanate method (Chomczynski and Sacchi 1987). RNA samples (50 μg) were assayed for the presence of *BMP-7* mRNA using two *BMP-7*-specific riboprobes: a 220-bp fragment from sequences corresponding to exon 1 (nucleotides 321–541) and a 202-bp fragment corresponding to a *StuI–StuI* fragment (nucleotides 884–1082 of the *mBMP-7* cDNA subcloned into pBluescript-KS). This region encodes sequences immediately adjacent to the mature region. A riboprobe that detects a fragment of the Sp1 transcription factor mRNA was used as a control for RNA loading (gift from Daniel Constam, Harvard University, Cambridge, MA). RNase protection was carried out as described (Ausubel et al. 1987) except that probes were labeled with [^{32}P]-UTP (800 mCi/mmole,) and hybridization was at 65°C.

Histology and in situ hybridization

Animals were sacrificed by asphyxiation with halothane. Tissues were fixed in 4% paraformaldehyde in PBS at 4°C overnight, followed by dehydration through a graded ethanol series. The material was cleared in xylene and embedded in a 1:1 ratio of Paraplast Plus and Tissue Prep 2 (Fisher) paraffin wax. Samples were sectioned at 6 μm, and sections collected on Tespa-treated glass slides. Sections for histology were stained with hematoxylin and eosin using standard procedures.

In situ hybridization was performed as described (Jones et al. 1991). Probes specific for *BMP-7* (Lyons et al. 1995), *Pax-2* (Dressler et al. 1990), *Pax-8* (Plachov et al. 1990), *Wnt-4* (Stark et al. 1994), *c-ret* (Pachnis et al. 1993), *msx-1* (Monaghan et al. 1991), and *Pax-6* (Walther and Gruss 1991) were used as described. Sections were photographed using a Leitz DMR photomicroscope and Ektachrome 160T color slide film.

Skeleton preparations

Skeletal staining was performed as described (McLeod 1980), with the following modifications. Skeletons were stained overnight at 37°C, washed in 1% KOH for 1 hr, and then transferred to 1% KOH for 24–48 hr at room temperature. The material was transferred through 20%, 50%, and 100% glycerol/1% KOH before final storage in 100% glycerol.

Acknowledgments

References

Ausubel, F.M., R. Brent, R.E. Kingston, D.D. Moore, J.G. Seidman, J.A. Smith, and K. Struhl eds. 1987. Ribonuclease protection assay. In *Current protocols in molecular biology*, pp. 4.7.1. John Wiley & Sons/Greene, New York.

Bradley, A. 1987. Production and analysis of chimeric mice. In *Teratocarcinomas and embryonic stem cells; a practical approach* ed. E.J. Robertson, pp. 131–151. IRL Press, Oxford, UK.

Celeste, A.J., J.A. Iannazzi, R.C. Taylor, R.M. Hewick, V. Rosen, E.A. Wang, and J.M. Wozney. 1990. Identification of transforming growth factor β family members present in bone-inductive protein purified from bovine bone. *Proc. Natl. Acad. Sci.* **87:** 9843–9847.

Chase, H.B. and E.B. Chase. 1941. Studies on an anophthalmic strain of mice. I. Embryology of the eye region. *J. Morphol.* **68:** 279–301.

Chomczynski, P. and N. Sacchi. 1987. Single-step method of RNA isolation by acid guanidinium thiocyanate–phenol–chloroform extraction. *Anal. Biochem.* **162:** 156–159.

Coles, H.S.R., J.F. Burne, and M.C. Raff. 1993. Large-scale normal cell death in the developing rat kidney and its reduction by epidermal growth factor. *Development* **118:** 777–784.

Conlon, F.L., K.M. Lyons, N. Takaesu, K.S. Barth, A. Kispert, B. Herrmann, and E.J. Robertson. 1994. A primary requirement for *nodal* in the formation and maintenance of the primitive streak in the mouse. *Development* **120:** 1919–1928.

Dressler, G. R., U. Deutsch, K. Chowdhury, H.O. Nornes, and P. Gruss. 1990. *Pax2*, a new murine paired-box containing gene and its expression in the developing excretory system. *Development* **109:** 787–795.

Ferguson, E.L. and K.V. Anderson. 1992. *Decapentaplegic* acts as a morphogen to organize dorsal-ventral pattern in the *Drosophila* embryo. *Cell* **71:** 451–461.

Francis, P.H., M.K. Richardson, P.M. Brickell, and C. Tickle. 1994. Bone morphogenetic proteins and a signaling pathway that controls patterning in the developing limb bud. *Development* **120:** 209–218.

Gelbart, W.M. 1989. The decapentaplegic gene: A TGF-β homologue controlling pattern formation in *Drosophila. Development* (Suppl.) **107:** 65–74.

Glaser, T., D.S. Walton, J. Cai, J.A. Epstein, L. Jepeal, and R.L. Maas. 1995. *PAX6* gene mutations in Aniridia. In *Molecular genetics of ocular disease* (ed. J. Wiggs), pp. 51–82. Wiley-Liss, New York.

Graham, A., P. Francis-West, P. Brickell, and A. Lumsden. 1994. The signaling molecule BMP4 mediates apoptosis in the rhombencephalic neural crest. *Nature* **372:** 684–686.

Grainger, R.M. 1992. Embryonic lens induction: Shedding light on vertebrate tissue determination. *Trends Genet.* **8:** 349–355.

Green, M.C. 1968. Mechanism of the pleiotropic effects of the

short ear mutant gene in the mouse. *J. Exp. Zool.* **167:** 129–150.

Grindley, J.C., D.R. Davidson, and R.E. Hill. 1995. The role of *Pax-6* in eye and nasal development. *Development* **121:** 1433–1442.

Harch, C., H.B. Chase, and N.I. Gonsalves. 1978. Studies on an anophthalmic strain of mice. *Dev. Biol.* **63:** 352–357.

Harland, R.M. 1994. The transforming growth factor β family and induction of the vertebrate mesoderm: Bone morphogenetic proteins are ventral inducers. *Proc. Natl. Acad. Sci.* **91:** 10243–10246.

Heberlein, U. and K. Moses. 1995. Mechanisms of *Drosophila* retinal morphogenesis: The virtues of being progressive. *Cell* **81:** 987–990.

Hill, R.E., J. Favor, B.L.M. Hogan, C.C.T. Ton, G.F. Saunders, I.M. Hanson, J. Prosser, T. Jordan, N.D. Hastie, and V. van Heyningen. 1991. Mouse *small eye* results from mutations in a paired-like homeobox-containing gene. *Nature* **354:** 522–525.

Hogan, B.L.M., E.M.A. Hirst, G. Horsburgh, and C.M. Hetherington. 1988. *Small eye* (*Sey*): A mouse model for the genetic analysis of craniofacial abnormalities. *Development* (Suppl.) **103:** 115–119.

Jones, C.M., K.M. Lyons, and B.L.M. Hogan. 1991. Involvement of bone morphogenetic protein-4 (*BMP-4*) and *Vgr-1* in morphogenesis and neurogenesis in the mouse. *Development* **111:** 531–542.

Kessler, D.S. and D.A. Melton. 1994. Vertebrate embryonic induction: Mesodermal and neural patterning. *Science* **226:** 596–604.

King, J.A., P.C. Marker, K.J. Seung, and D.M. Kingsley. 1994. *BMP5* and the molecular, skeletal, and soft-tissue alterations in *short ear* mice. *Dev. Biol.* **166:** 112–122.

Kingsley, D.M. 1994. The TGF-β superfamily; new members, new receptors and new genetic tests of function in different organisms. *Genes & Dev.* **8:** 133–146.

Kingsley, D.M., A.E. Bland, J.M. Grubber, P.C. Marker, L.B. Russell, N.G. Copeland, and N.A. Jenkins. 1992. The mouse *short ear* skeletal morphogenesis locus is associated with defects in a bone morphogenetic member of the TGFβ superfamily. *Cell* **71:** 399–410.

Koseki, C., D. Herzlinger, and Q. Al-Awqati. 1992. Apoptosis in metanephric development. *J. Cell Biol.* **119:** 1327–1333.

Liu, F., F. Ventura, J. Doody, and J. Massague. 1995. Human type II receptor for bone morphogenetic proteins (BMPs): Extension of the two-kinase receptor model to the BMPs. *Mol. Cell. Biol.* **15:** 3479–3486.

Lyon, M.F. and A.G. Searle. 1989. *Genetic variants and strains of the laboratory mouse*, 2nd Ed. Oxford University Press, Oxford, UK.

Lyons, K.M., R.W. Pelton, and B.L. Hogan. 1989. Patterns of expression of murine *Vgr-1* and *BMP-2a* RNA suggest that transforming growth factor-β-like genes coordinately regulate aspects of embryonic development. *Genes & Dev.* **3:** 1657–1668.

———. 1990. Organogenesis and pattern formation in the mouse: RNA distribution patterns suggest a role for bone morphogenetic protein-2A (*BMP-2A*). *Development* **109:** 833–844.

Lyons, K.M., C.M. Jones, and B.L.M. Hogan. 1991. The DVR gene family in embryonic development. *Trends Genet.* **7:** 408–412.

Lyons, K.M., B.L.M. Hogan, and E.J. Robertson. 1995. Colocalization of *BMP 7* and *BMP 2* RNAs suggests that these factors cooperatively mediate tissue interactions during murine development. *Mech. Dev.* **50:** 71–83.

McLeod, M.J. 1980. Differential staining of cartilage and bone in whole mouse fetuses by alcian blue and alizarine red S. *Teratology* **22:** 299–301.

Monaghan, A.P., D.R. Davidson, C. Sime, E. Graham, R. Baldock, S.S. Bhattacharya, and R.E. Hill. 1991. The *Msh*-like homeobox genes define domains in the developing vertebrate eye. *Development* **112:** 1053–1061.

Niswander, L. and G.R. Martin. 1993. FGF-4 and BMP-2 have opposite effects on limb growth. *Nature* **361:** 68–71.

Özkaynak, E., D.C. Rueger, E.A. Drier, C. Corbett, R.J. Ridge, T.K. Sampath, and H. Oppermann. 1990. *OP-1* cDNA encodes an osteogenic protein in the TGF-β family. *EMBO J.* **9:** 2085–2093.

Özkaynak, E., P.N.J. Schnegelsbert, and H. Oppermann. 1991. Murine osteogenic protein (OP-1): High levels of mRNA in kidney. *Biochem. Biophys. Res. Commun.* **179:** 116–123.

Pachnis, V., B. Mankoo, and F.C. Costantini. 1993. Expression of the *c-ret* proto-oncogene during mouse embryogenesis. *Development* **119:** 1005–1017.

Padgett, R.W., R.D. St Johnson, and W.M. Gelbart. 1987. A transcript from a *Drosophila* pattern gene predicts a protein homologous to the transforming growth factor-β family. *Nature* **325:** 81–84.

Padgett, R.W., J. Wozney, and W.M. Gelbart. 1993. Human BMP sequences can confer normal dorsal-ventral patterning in the *Drosophila* embryo. *Proc. Natl. Acad. Sci.* **90:** 2905–2909.

Plachov, D., K. Chowdhury, C. Walther, D. Simon, J.L. Guenet, and P. Gruss. 1990. *Pax8*, a murine paired box gene expressed in the developing excretory system and thyroid gland. *Development* **110:** 643–651.

Poirier, F. and E.J. Robertson. 1993. Normal development of mice carrying a null mutation in the gene encoding the L14 S-type lectin. *Development* **119:** 1229–1236.

Rabacchi, S.A., L. Bonfanti, X-H. Liu, and L. Maffei. 1994. Apoptotic cell death induced by optic nerve lesion in the neonatal rat. *J. Neurosci.* **14:** 5292–5301.

Ramirez-Solis, R., A.C. Davis, and A. Bradley. 1993. Gene targeting in embryonic stem cells. *Methods Enzymol.* **225:** 855–877.

Robertson, E., A. Bradley, M. Kuehn, and M. Evans. 1986. Germ line transmission of genes introduced into cultured pluripotential cells by retroviral vector. *Nature* **323:** 445–448.

Rosen, V. and R.S. Thies. 1992. The BMP proteins in bone formation and repair. *Trends Genet.* **8:** 97–102.

Rosenzweig, B.L., T. Imamura, T. Okadome, G.N. Cox, H. Yamashita, P. ten Dijke, C.-H. Heldin, and K. Mityazono. 1995. Cloning and characterization of a human type II receptor for bone morphogenetic proteins. *Proc. Natl. Acad. Sci.* **92:** 7632–7636.

Sampath, T.K., K.E. Rashka, J.S. Doctor, R.F. Tucker, and F.M. Hoffmann. 1993. *Drosophila* transforming growth factor beta superfamily proteins induce endochondral bone formation in mammals. *Proc. Natl. Acad. Sci.* **90:** 6004–6008.

Sanyanusin, P., L.A. Schimmenti, L.A. McNoe, T.A. Ward, M.E.M. Pierpont, M.J. Sullivan, W.B. Dobyns, and M.R. Eccles. 1995. Mutation of the *PAX2* gene in a family with optic nerve colobomas, renal anomalies and vesicoureteral reflux. *Nature Genet.* **9:** 358–364.

Saxen, L. 1987. *Organogenesis of the kidney* (ed. P.W. Barlow, P.B. Green and C.C. White), Vol. 19, Cambridge University Press, Cambridge, UK.

Schuchardt, A., V. D'Agati, L. Larsson-Blomberg, F. Costantini, and V. Pachnis. 1994. Defects in the kidney and enteric nervous system of mice lacking the tyrosine kinase receptor *Ret. Nature* **367:** 380–383.

Silver, J. and R.M. Robb. 1979. Studies on the development of

the eye cup and optic nerve in normal mice and in mutants with congenital optic nerve aplasia. *Dev. Biol.* **68:** 175–190.

Stark, K., S. Vainio, G. Vassileva, and A.P. McMahon. 1994. Epithelial transformation of metanephric mesenchyme in the developing kidney regulated by *Wnt-4*. *Nature* **372:** 679-683.

Tabin, C. 1995. The initiation of the limb bud: Growth factors, Hox genes and retinoids. *Cell* **80:** 671–674.

Theiler, K., D.S. Varnum, and L.C. Stevens. 1978. Development of Dickie's Small eye, a mutation in the house mouse. *Anat. Embryol.* **155:** 81–86.

Vainio, S., I. Karavanova, A. Jowett, and I. Thesleff. 1993. Identification of BMP-4 as a signal mediating secondary induction between epithelial and mesenchymal tissues during early tooth development. *Cell* **75:** 45–58.

Vukicevic, S., V. Latin, P. Chen, R. Batorsky, A.H. Reddi, and T.K. Sampath. 1994. Localization of osteogenic protein-1 (bone morphogenetic protein-7) during human embryonic development: High affinity binding to basement membranes. *Biochem. Biophys. Res. Commun.* **198:** 693–700.

Walther, C. and P. Gruss. 1991. *Pax-6*, a murine paired box gene, is expressed in the developing CNS. *Development* **113:** 1435–1449.

Walther, C., J.-L. Guenet, D. Simon, U. Deutsch, B. Jostes, M. Goulding, D. Plachov, R. Balling, and P. Gruss. 1991. Pax: A multigene family of paired box-containing genes. *Genomics* **11:** 424–434.

Wessells, N.K. 1977. *Tissue interactions and development.* W.A. Benjamin, Inc., Menlo Park, California.

Wharton, K.A., G.H. Thomsen, and W.M. Gelbart. 1991. *Drosophila 60A* gene, another transforming growth factor beta family member, is closely related to human bone morphogenetic proteins. *Proc. Natl. Acad. Sci.* **88:** 9214–9218.

Winnier, G., M. Blessing, P.A. Labosky, and B.L.M. Hogan. 1995. Bone morphogenetic protein-4 (*BMP-4*) is required for mesoderm formation and patterning in the mouse. *Genes & Dev.* **9:** 2105–2117.

Wozney, J.M., V. Rosen, A.J. Celeste, L.M. Mitsock, M.J. Whitters, R.W. Kriz, R.M. Hewick, and E. Wang. 1988. Novel regulators of bone formation: Molecular clones and activities. *Science* **242:** 1528–1534.

Yamashita, H., P. ten Dijke, D. Huylebroeck, T.K. Sampath, M. Andries, J.C. Smith, C.-H. Heldin, and K. Miyazono. 1995. Osteogenic protein-1 binds to activin type II receptors and induces certain activin-like effects. *J. Cell Biol.* **130:** 217–226.

Zhou, X., H. Sasaki, L. Lowe, B.L.M. Hogan, and M.R. Kuehn. 1993. *Nodal* is a novel TGF-β-like gene expressed in the mouse node during gastrulation. *Nature* **361:** 543–547.

A requirement for bone morphogenetic protein-7 during development of the mammalian kidney and eye.

A T Dudley, K M Lyons and E J Robertson

References	This article cites 60 articles, 28 of which can be accessed free at: **http://genesdev.cshlp.org/content/9/22/2795.full.html#ref-list-1**
License	
Email Alerting Service	Receive free email alerts when new articles cite this article - sign up in the box at the top right corner of the article or **click here.**